Nitric Oxide 88 (2019) 73–86

Contents lists available at ScienceDirect

Nitric Oxide

journal homepage: www.elsevier.com/locate/yniox

Characterization of plant glutamine synthetase S-nitrosation

Liliana S. Silva[a,b,c], Mariana Q. Alves[a], Ana R. Seabra[c], Helena G. Carvalho[a,b,c,*]

[a] IBMC, Instituto de Biologia Molecular e Celular da Universidade do Porto; i3S, Instituto de Investigação e Inovação em Saúde, Universidade do Porto, Rua Alfredo Allen, 4200-135 Porto, Portugal

[b] Faculdade de Ciências da Universidade do Porto, Rua do Campo Alegre, s/n, 4169-007 Porto, Portugal

[c] Centro de Investigação em Biodiversidade e Recursos Genéticos da Universidade do Porto, Campus de Vairão, Rua Padre Armando Quintas, No 7, 4485-661, Vairão, Portugal

ARTICLE INFO

Keywords:
Glutamine synthetase
Nitric oxide
Medicago truncatula
S-nitrosation
Root nodule

ABSTRACT

The identification of *S*-nitrosated substrates and their target cysteine residues is a crucial step to understand the signaling functions of nitric oxide (NO) inside the cells. Here, we show that the key nitrogen metabolic enzyme glutamine synthetase (GS) is a *S*-nitrosation target in *Medicago truncatula* and characterize the molecular determinants and the effects of this NO-induced modification on different GS isoenzymes. We found that all the four *M. truncatula* GS isoforms are *S*-nitrosated, but despite the high percentage of amino acid identity between the four proteins, *S*-nitrosation only affects the activity of the plastid-located enzymes, leading to inactivation. A biotin-switch/mass spectrometry approach revealed that cytosolic and plastid-located GSs share an *S*-nitrosation site at a conserved cysteine residue, but the plastidic enzymes contain additional *S*-nitrosation sites at non-conserved cysteines, which are accountable for enzyme inactivation. By site-directed mutagenesis, we identified Cys369 as the regulatory *S*-nitrosation site relevant for the catalytic function of the plastid-located GS and an analysis of the structural environment of the SNO-targeted cysteines in cytosolic and plastid-located isoenzymes explains their differential regulation by *S*-nitrosation and elucidates the mechanistic by which *S*-nitrosation of Cys369 leads to enzyme inactivation. We also provide evidence that both the cytosolic and plastid-located GSs are endogenously *S*-nitrosated in leaves and root nodules of *M. truncatula*, supporting a physiological meaning for *S*-nitrosation. Taken together, these results provide new insights into the molecular details of the differential regulation of individual GS isoenzymes by NO-derived molecules and open new paths to explore the biological significance of the NO-mediated regulation of this essential metabolic enzyme.

1. Introduction

Nitric oxide (NO) is a key-signaling messenger in plants, being involved in a wide variety of physiological processes, ranging from normal plant growth and developmental processes to responses to biotic and abiotic stresses [1,2]. The biological effect of NO is mainly achieved through a direct interaction with specific atoms of target proteins, inducing post-translational modifications (PTMs), such as *S*-nitrosation, commonly referred to as S-nitrosylation, and tyrosine nitration, which can impact protein functionality, stability and subcellular localization [3]. Protein *S*-nitrosation, the reversible covalent attachment of the NO moiety to thiol groups of selected cysteine residues, is considered the major route for the transfer of NO bioactivity in plants [4,5]. Up to date, hundreds of plant proteins have been reported to undergo *S*-nitrosation, including enzymes involved in vital metabolic processes, such as photosynthesis, photorespiration, carbon and nitrogen metabolism [6–19]. In spite of the increasing number of *S*-nitrosation targets identified in plants, the molecular details and the physiological effects of *S*-nitrosation are only known for a few proteins and it is extremely important to extend this knowledge, to better understand the molecular mechanisms underlying the signaling events mediated by NO.

We have previously shown that glutamine synthetase (GS) is modulated by NO, being subjected to tyrosine nitration and possibly *S*-nitrosation, but in an isoenzyme specific manner [20]. The regulation of GS by NO is particularly interesting because the production of NO is necessarily linked to nitrogen (N) metabolism in which GS occupies a central position. GS catalyzes the first step in nitrogen assimilation, the ATP-dependent ligation of ammonia and glutamate to yield glutamine (see eq. (1)), which is then used as a building block for the biosynthesis

* Corresponding author. Centro de Investigação em Biodiversidade e Recursos Genéticos da Universidade do Porto, Campus de Vairão, Rua Padre Armando Quintas, No 7, 4485-661, Vairão, Portugal.
E-mail address: helenacarvalho@cibio.up.pt (H.G. Carvalho).

https://doi.org/10.1016/j.niox.2019.04.006
Received 14 February 2019; Received in revised form 5 April 2019; Accepted 13 April 2019
Available online 23 April 2019

of essentially all N-containing biomolecules.

$$\text{Glutamate} + \text{Ammonia} + \text{ATP} \xrightarrow[\text{GS}]{} \text{Glutamine} + \text{ADP} + \text{Pi} + H_2O \quad (1)$$

Given its critical role, GS is ubiquitous and well conserved across all domains of life, from unicellular organisms to mammals, and considered one the oldest functioning enzymes [21,22]. In higher plants, GS catalyzes the first step of N assimilation and is also involved in the reassimilation of the ammonium constantly released by a number of metabolic pathways. GS exists in the plant as a number of decameric isoenzymes, which share a high degree of amino acid conservation and are located both in the cytosol (GS1) and in the plastids (GS2) and are encoded by a small family of genes. In the case of the model legume *M. truncatula,* GS is encoded by four different genes: *MtGS1a* and *MtGS1b* encoding cytosolic polypeptides of 39 kDa; and *MtGS2a* and *MtGS2b*, encoding plastid-located polypeptides of 42 kDa [23]. Specific GS isoenzymes are differentially expressed in different organs and cell types to assimilate the ammonium produced by different physiological processes. The most abundantly expressed isoenzymes are, by far, MtGS1a and MtGS2a. MtGS1a is highly expressed in root nodules where it functions to assimilate the ammonium released by nitrogen fixing bacterial symbionts [24] and MtGS2a is very abundant in all photosynthetic tissues being mainly involved in the reassimilation of ammonium released during photorespiration but also involved in the primary assimilation of the ammonium derived from nitrate reduction [25]. The cytosolic MtGS1b appears to play a housekeeping role and is ubiquitously expressed in all organs of the plant at moderate levels, however its expression considerably increases during senescence and presumably is the isoenzyme responsible for the reassimilation of the ammonia derived from protein catabolism [23,26,27]. MtGS2b is exclusively expressed in the seeds and is unique to *M. truncatula* and closely related species [28].

The central position occupied by GS in plant N metabolism implies that both its synthesis and activity must be strictly regulated. Post-translational modifications are highly important for the regulation of GS activity, as they can, reversibly or irreversibly, modulate enzyme activity and function, providing a short-term response to sudden metabolic or environmental fluctuations. It has been shown that plant GS can suffer a number of PTMs including phosphorylation [29–31], oxidation [32] tyrosine nitration [20,33], methionine sulfoxidation [33] and possibly *S*-nitrosation [20]. However, not much is known about the molecular details and physiological significance of these PTMs, especially in what concerns the regulation of GS by *S*-nitrosation.

S-nitrosation is considered a selective process determined by several protein structural factors but also by the proximity of the target to a bioavailable NO source [34,35]. The extent of *S*-nitrosation of a given protein will be determined by the balance between the rates of *S*-nitrosation and denitrosation. *S*-nitrosoglutathione (GSNO), resulting from the reaction of NO with GSH, is a major *S*-nitrosation agent in the cell, and its intracellular levels are determined by the balance between its synthesis and degradation [36,37]. Although the mechanisms of GSNO synthesis in plants are still not clearly elucidated [5], it is well known that it is irreversibly degraded by GSNO reductase (GSNOR) [38]. GSNOR catalyzes the reduction of GSNO to oxidized glutathione (GSSG) releasing ammonium and it has been recently shown that the enzyme is itself *S*-nitrosated at Cys10, which induces local conformational changes exposing an autophagy-related-interacting motif causing selective autophagy and resulting in increased NO concentration under hypoxia conditions [39]. It is noteworthy that GSNOR has been implicated in many important NO-regulated processes such as root development and pathogen defense and also N assimilation [40–42]. As the ammonium produced by GSNOR is inevitably assimilated by GS, the activity of the two enzymes is necessarily linked and thus the regulation of GS by *S*-nitrosation is worth investigating.

In this study, we investigate the regulation of GS by *S*-nitrosation in *M. truncatula* and we show that all the four *M. truncatula* GS isoenzymes are susceptible to *S*-nitrosation *in vitro*, but with different outcomes for GS activity. We show that the plastid-located enzymes are inhibited by *S*-nitrosation, identify the regulatory residue and provide a structural interpretation for the differential regulation of cytosolic and plastid GSs by *S*-nitrosation. In addition, we demonstrate that both the cytosolic and the plastid-located GSs are endogenously *S*-nitrosated under physiological conditions.

2. Material and methods

2.1. Materials

All reagents were purchased from Sigma-Aldrich unless otherwise specified.

2.2. Plant material and growth conditions

M. truncatula Gaertn (cv. Jemalong J5) was grown in aeroponic conditions under 16 h light (22 °C)/8 h dark (19 °C) cycles and under a light intensity of 150–200 μmol m^{-2} s^{-1}, in a medium supplemented with 5 mM NH_4NO_3 as described by Lullien et al. [43]. For nodule induction, the nutrient solution was replaced with fresh nitrogen-free medium three days before inoculation with *Sinorhizobium meliloti* strain Rm1021 SU 47 (2011), str-21 [44]. Nodules were harvested 21 days after inoculation. Leaves were collected from plants grown on soil and fertilized once a week. All plant material was immediately frozen in liquid nitrogen and stored at −80 °C.

2.3. Purification of recombinant GS isoenzymes

The *M. truncatula* GS isoenzymes MtGS1a, MtGS1b, MtGS2a, and MtGS2b were produced in *Escherichia coli* BL21-CodonPlus (DE3)-RP cells harboring previously described gene constructs MtGS1a:pET24d; MtGS1b:pET24d, MtGS2a:pET24d and MtGS2b:pET24d encoding C-terminal His_6-tagged fusion proteins [45]. Expression of the recombinant proteins was induced with isopropyl β-D-1-thiogalactopyranoside (IPTG) (final concentration 0.1 mM) at mid-exponential growth ($O.D._{600nm}$ = 0.5) and cell growth continued overnight at 20 °C. The cells were harvested by centrifugation at 2800*g* and resuspended in extraction buffer (50 mM sodium phosphate buffer, pH 8; 0.5 M NaCl; 5 mM $MgSO_4$; 5 mM sodium glutamate and 2 mM β-mercaptoethanol) supplemented with 200 μg mL^{-1} lysozyme, disrupted by sonication and centrifuged (30 min, 20000 *g*, 4 °C) to remove cell debris. Recombinant GSs were purified under native conditions by Ni-affinity chromatography (Ni-NTA His-bind resin) following the supplier's instruction (Novagen, Millipore). Proteins were eluted in buffer A (50 mM sodium phosphate buffer, pH 7.5; 5 mM $MgSO_4$; 5 mM sodium glutamate) containing 300 mM imidazole and dialyzed against buffer A containing 0.5 mM β-mercaptoethanol. Protein concentration was determined using a Nanodrop spectrophotometer (Thermo Scientific™) and protein purity confirmed by sodium dodecyl sulfate polyacrylamide gel electrophoresis (SDS-PAGE).

2.4. Determination of GS activity

GS activity was determined spectrophotometrically by measuring the formation of γ-glutamyl hydroxamate as described by Cullimore and Sims [46]. The activity of the recombinant enzymes MtGS1a, MtGS1b and MtGS2a was determined by the transferase reaction and the activity of MtGS2b by the biosynthetic reaction, because the enzyme has low transferase activity [28]. One unit of activity is equivalent to γ-glutamyl hydroxamate at 1 μmol min^{-1} produced per total amount of protein (μg^{-1}) at 30 °C.

2.5. In vitro S-nitrosation assays

Purified recombinant proteins were *in vitro S*-nitrosated by incubation with the stated concentration of *S*-nitrosoglutathione (GSNO), at room temperature for 30 min in darkness. Parallel assays were performed using GSH, instead of GSNO, to serve as control. The concentration of GSNO was determined before each experiment by UV/VIS spectrophotometry at 335 nm (ε_{335} = 922 $M^{-1}cm^{-1}$) [47]. The protein concentration in the assays was 25 ng μL^{-1} for MtGS1a or MtGS1b and 50 ng μL^{-1} for MtGS2a or MtGS2b. The resulting proteins were subjected to GS activity measurements and to the biotin-switch technique.

2.6. Protein extraction from plant tissues

Plant material was homogenized at 4 °C in a mortar and pestle in 2 vol of extraction buffer (50 mM Hepes-NaOH, pH 7.7; 5 mM EDTA; 0.5 mM neocuproine; 0.5% (v/v) Triton™ X-100 and 0.5% (v/v) protease inhibitor cocktail for plant cell extracts), centrifuged at 20000 *g* for 20 min at 4 °C and the soluble fraction was recovered. Protein concentration was measured by the Coomassie dye binding assay (BioRad, Lda) using bovine serum albumin as a standard.

2.7. Biotin-switch technique (BST)

S-nitrosated proteins were detected using the biotin switch technique according to Jaffrey et al. [48] with minor modifications. Protein extracts were diluted to 0.8 µg μL^{-1} in HEN buffer (50 mM Hepes-NaOH, pH 7.7; 5 mM EDTA; 0.5 mM neocuproine) and incubated with *S*-methyl-methanethiosulfonate (MMTS) (final concentration 20 mM) and 2.5% (w/v) SDS for 20 min at 50 °C with frequent vortexing. Unreacted MMTS was removed by acetone precipitation at − 20 °C and the proteins resuspended in HENS buffer (HEN buffer containing 1% (w/v) SDS). After addition of 0.1 mM biotin-HPDP (Thermo Scientific™) and 50 mM sodium ascorbate, the mixture was incubated for 3 h at room temperature in the dark and frequently vortexed. The excess of ascorbate and biotin-HPDP was removed by acetone precipitation and the biotinylated proteins were purified by avidin-affinity chromatography. Biotinylated samples were diluted in 5 vol of neutralization buffer (20 mM Hepes-NaOH, pH 7.7; 150 mM NaCl; 5 mM EDTA; 0.5% (v/v) Triton™ X-100) supplemented with 20 µL neutravidin-agarose (Pierce biotechnology, Thermo Scientific™) and incubated for 1 h at room temperature, with gentle shaking. The matrix with bound proteins was washed several times in 200 µL washing buffer (20 mM Hepes-NaOH, pH 7.7; 750 mM NaCl; 5 mM EDTA; 0.5% (v/v) Triton™ X-100) and transferred to an empty tube. Finally, the biotinylated proteins were eluted by incubation for 5 min at 95 °C in SDS-PAGE sample buffer, supplemented with 100 mM β-mercaptoethanol and analyzed by immunoblotting with the appropriate antibodies.

For the detection of *in vivo S*-nitrosated proteins 1 mg of total soluble leaf proteins or 300 µg of nodule proteins was used as starting material. For the detection of *in vitro S*-nitrosated GS, 10 µg of each recombinant protein was first treated with 500 µM GSH or GSNO for 30 min at room temperature. The GS samples were then desalted using PD MiniTrap G-25 columns (GE Healthcare, Lifesciences) and assayed for biotin-switch as described above.

2.8. MALDI-TOF/TOF and mass spectrometry analysis

For nLC-MS/MS and MALDI-TOF/TOF analysis, biotin-labeled proteins were resolved by 12% (w/v) SDS-PAGE under non-reducing conditions and stained with BlueSafe (NZYtech, Lda) according to the manufacturer's instructions. The proteins were excised from the gel and digested with trypsin (sequencing grade; Promega, Madison, WI, USA) according to Osorio and Reis [49] with minor alterations. The protein gel plugs were washed with water, destained with methanol/50 mM NH_4HCO_3 and acetonitrile/50 mM NH_4HCO_3 (1:1 v/v each) and in-gel digested, under non-reducing conditions, with 10 µL of 2 ng μL^{-1} trypsin for 3 h at 37 °C in the presence of 0.01% (v/v) surfactant (ProteaseMAX, Promega), and the resulting peptides were extracted with 20 µL of TFA 2.5% (v/v) for 15 min. Peptides were then desalted, concentrated using reversed phase micro-columns ZipTip® (Millipore, Bedford, MA, USA) according to the manufacturer protocol.

Protein identification was performed by nanoLC-MS/MS. This equipment was composed by an Ultimate 3000 liquid chromatography system coupled to a Q-Exactive Hybrid Quadrupole-Orbitrap mass spectrometer (Thermo Scientific™, Bremen, Germany). Samples were resuspended in formic acid (0.1%) and loaded onto a trapping cartridge (Acclaim PepMap C18 100Å, 5 mm × 300 µm i. d., 160454, Thermo Scientific™) in a mobile phase of 2% ACN, 0.1% FA at 10 µL min^{-1}. After 3 min loading, the trap column was switched in-line to a 50 cm by 75 µm inner diameter EASY-Spray column (ES803, PepMap RSLC, C18, 2 µm, Thermo Scientific™, Bremen, Germany) at 300 nl min^{-1}. Separation was generated by mixing A: 0.1% FA, and B: 80% ACN, with the following gradient: 5 min (2.5% B to 10% B), 120 min (10% B to 30% B), 35 min (30% B to 50% B), 3 min (50%–99% B) and 12 min (hold 99% B). Subsequently, the column was equilibrated with 2.5% B for 12 min. Data acquisition was controlled by Xcalibur 4.0 and Tune 2.9 software (Thermo Scientific™, Bremen, Germany).

The mass spectrometer was operated in data-dependent (dd) positive acquisition mode alternating between a full scan (*m/z* 380–1580) and subsequent HCD MS/MS of the 10 most intense peaks from full scan (normalized collision energy of 27%). ESI spray voltage was 1.9 kV and capillary temperature was 275 °C. Global settings: use lock masses best (*m/z* 445.12003), lock mass injection Full MS, chrom. peak width (FWHM) 15 s. Full scan settings: 70k resolution (*m/z* 200), AGC target 3e6, maximum injection time 120 ms dd settings: minimum AGC target 7e3, intensity threshold 2.8e4, charge exclusion: unassigned, 1, 8, > 8, peptide match preferred, exclude isotopes on, dynamic exclusion 45s. MS2 settings: microscans 1, resolution 35k (*m/z* 200), AGC target 2e5, maximum injection time 250 ms, isolation window 2.0 *m/z*, isolation offset 0.0 *m/z*, spectrum data type profile.

The raw data was processed using Proteome Discoverer 2.2.0.388 software (Thermo Scientific™) and searched against the UniProt database for the *Medicago truncatula* taxonomic selection (2018_09 release). The Sequest HT search engine was for protein identification. The ion mass tolerance was 10 ppm for precursor ions and 0.02 Da for fragment ions. Maximum allowed missing cleavage sites was set 2. Cysteine carbamidomethylation was defined as constant modification. Methionine oxidation, cysteine methylthio, cysteine biotin-HPDP, and protein N-terminus acetylation were defined as variable modifications. Peptide confidence was set to high. The processing node Percolator was enabled with the following settings: maximum delta Cn 0.05; decoy database search target FDR 1%, validation was based on q-value.

For the MALDI-TOF/TOF analysis, samples were crystallized onto a MALDI plate with a solution of 5–10 mg mL^{-1} α-cyano-4-hydroxycinnamic acid in 50% (v/v) acetonitrile/0.1% (v/v) trifluoroacetic acid. Samples were analyzed using a 4800 Plus MALDI-TOF/TOF Analyzer (AB SCIEX, Framingham, MA). Peptide mass fingerprint (PMF) data was collected in positive MS reflector mode in the range of 500–5000 (*m/z*) and was calibrated internally using trypsin autolysis peaks. MS spectra were processed and analyzed using the software GPS Explorer (Version 3.6, AB SCIEX, Framingham, MA) and were searched together against the UniProt protein sequence database using the Mascot search engine (version 2.4, Matrix Science, London, UK) limited to *M. truncatula* taxonomy. The search was directed to the cysteine-containing peptides and up to two missed trypsin cleavage sites were allowed. The MS tolerance was 0.8 Da for MS/MS analysis; fixed modifications, “methylthio” (C); variable modifications, “biotin-HPDP” (C); keratins were filtered out. To be considered a match, a confidence interval (CI), calculated by the AB SCIEX GPS Explorer/Mascot software, of at least 99% was required.

2.9. Site-directed mutagenesis

The mutation of Cys304 and Cys369 to serine in MtGS2a was performed by site-directed mutagenesis using the NZYMutagenesis kit (NZYtech, Lda) following manufacturer's instructions. Single mutations were generated by PCR amplification using MtGS2a:pET24d plasmid [45] as template and primers containing the desired mutation. The sense sequences of the primers used are: C304S: 5' – GGTGATTGGAA TGGTGCA**GGGTCTCA**CACCAATTACAG – 3′ and C369S: 5' – GGAGTG GCTAACCGTGG**GAGCTC**AATCCGTGTG – 3′, where the underlined bases represent the nucleotide changes to mutate Cys304 (codon TGT) to Ser (codon TCT) or Cys369 (codon TGC) to Ser (codon AGC) and to create a *Sac*I or *Bsa*I restriction site (boldface), respectively, to facilitate the initial screening for mutation. The PCR amplified products were transformed into NZYStar Competent Cells (NZYtech, Lda) and the plasmid DNA was extracted and sequenced (StabVida, Portugal) to confirm the production of the desired mutations. The same procedure was used to obtain a double mutant (MtGS2aC304S/C369S) using MtGS2aC369S as template.

2.10. Gel electrophoresis, Western blot, and densitometric analysis

Proteins were separated by 12% (w/v) SDS-PAGE and electrotransferred onto nitrocellulose membranes (Whatman®) using a Criterion Blotter from BioRad, Lda. Immunodetection of GS polypeptides was performed using an anti-GLN1|GLN2 antibody AS08 295 (Agrisera) and a secondary goat anti-rabbit peroxidase conjugated antibody (Santa Cruz Biotechnology). Biotinylated BSA was detected using an anti-biotin peroxidase conjugate antibody (Agrisera). The immunocomplexes were detected by chemiluminescence using the ECL™ (GE Healthcare, Lifesciences) detection systems. The blots were imaged with the ChemiDoc MP imager (BioRad, Lda) and the band density in the blots was determined using the band analysis tools of ImageLab software version 4.1 (BioRad, Lda).

2.11. Structural analysis

MtGS1a coordinates and structural factors were downloaded from PDB (http://www.pdb.org) using the accession code 4is4 [50]. All images were generated using the PyMOL Molecular Graphics System, Version 2.0 Schrödinger, LLC.

2.12. Statistical analysis

Statistical analyses were performed using PRISM 7.0 software (GraphPad Software, San Diego, CA). Statistical significance was determined by Student's t-test, assuming equal variance. The results were considered significant if the p-value was < 0.05.

3. Results

3.1. S-nitrosation of individual M. truncatula GS isoenzymes

To evaluate the susceptibility to *S*-nitrosation of each individual member of the *M. truncatula* GS family, the plant proteins MtGS1a, MtGS1b, MtGS2a, and MtGS2b were independently produced in *E. coli* with a C-terminal His-tag and purified by Ni-affinity chromatography. The purified proteins were incubated with the trans-nitrosating agent *S*-nitrosoglutathione (GSNO) and subjected to the biotin-switch technique (BST). The biotin-labeled proteins were purified by avidin-affinity chromatography and analyzed by Western blot. This analysis revealed that all four *M. truncatula* GS isoenzymes are susceptible to *S*-nitrosation *in vitro*, as the four GS proteins are clearly detected following incubation with GSNO, but not when GSNO is replaced by GSH or when ascorbate is omitted (Fig. 1A - SNO). The strong signal detected in absence of the blocking agent MMTS results from labeling of all the cysteines present in the protein and serves as a positive control. Equal protein loading in each column is shown by the immunoblot detection of GS before avidin-affinity chromatography (Fig. 1A - GS).

The recombinant proteins were assayed for GS activity following incubation with increasing concentrations of GSNO or GSH in order to evaluate the impact of *S*-nitrosation on the activity of each individual isoenzyme. The activity of the two plastid-located enzymes MtGS2a and MtGS2b was found to be significantly reduced upon incubation with 100 µM and 500 µM GSNO, and the inactivation could be reversed by incubation with DTT (Fig. 1B). Conversely, the activity of the cytosolic isoenzymes MtGS1a and MtGS1b was not affected by incubation with the *S*-nitrosating agent (Fig. 1B). This is in accordance with a previous study on *M. truncatula* root nodule GS, which showed that both MtGS1a and MtGS2a are post-translationally modified by NO but the inhibitory effect induced by NO on the activity of the cytosolic enzyme is a consequence of tyrosine nitration whereas the inactivation of the plastid located enzyme results from oxidation of cysteine residue(s) [20]. Altogether, these results indicate that all four *M. truncatula* GS isoenzymes are prone to *S*-nitrosation, but only the activity of plastid-located enzymes is directly affected by this post-translational modification.

3.2. Identification of the S-nitrosation site(s) responsible for MtGS2a inactivation

GS contains several cysteine residues that can function as *S*-nitrosation sites, whose position within the primary amino acid sequences is shown in the alignment presented in Fig. 2. The cytosolic (MtGS1a and MtGS1b) and plastid-located (MtGS2a and MtGS2b) GSs share three conserved cysteine residues (positions 92, 159 and 179 in MtGS1a, and 148, 215 and 235 in MtGS2a), but the plastid-located enzymes contain two additional cysteine residues at positions 304 and 369. Interestingly, these two additional cysteine residues are absolutely conserved in all plant plastid-located enzymes and are placed at suitable positions to play a regulatory role as they integrate the GS conserved regions III and IV known to be important for the enzyme's catalytic activity (Fig. 2).

Taking into account that MtGS1a and MtGS2a share a similar decameric structure and a similar active site fold [50] but *S*–nitrosation only affects the activity of MtGS2a (Fig. 1), it is reasonable to assume that the relevant sites for the redox regulation of the catalytic function of MtGS2a are the cysteine residues exclusive of plastid-located isoenzymes (Cys304 and/or Cys369). To investigate if any of these residues is the regulatory *S*-nitrosation site(s), accountable for the specific susceptibility of MtGS2a to inactivation by *S*-nitrosation, Cys304 and Cys369 were mutated to serine by site-directed mutagenesis, independently (MtGS2aC304S, MtGS2aC369S) and as a double mutation (MtGS2aC304S/C369S), and the susceptibility of the mutated proteins to inactivation by GSNO was evaluated (Fig. 3). The mutated proteins contain a hydroxyl in place of the sulfhydryl group, thus mimicking the unmodified form of MtGS2a. The modified and unmodified proteins were expressed in *E. coli,* using the same expression and purification system, yielding around 15 mg L^{-1} of purified protein. The three mutant enzymes were found to be active and the specific activity of MtGS2aC369S was not too different from that of the non-mutated enzyme, however the substitution of Cys304 to serine lead to a significant reduction in specific activity, observed for the single mutant MtGS2aC304S as well as for the double mutant MtGS2aC304S/C369S (Fig. 3A). Conversely, the resistance to GSNO-induced inactivation was exclusively observed for the proteins mutated in Cys369. The proteins in which Cys369 was replaced by serine, either as a single (MtGS2aC369S) or double mutation (MtGS2aC304S/C369S) were found to be 20% more resistant to the GSNO induced inactivation when compared to the wild type protein, whereas the inhibition observed in MtGS2aC304S was comparable to the wild type protein (Fig. 3B). Taken together these results indicate that the inhibitory effects of GSNO on MtGS2a are mainly due to *S*-nitrosation of Cys369, and although

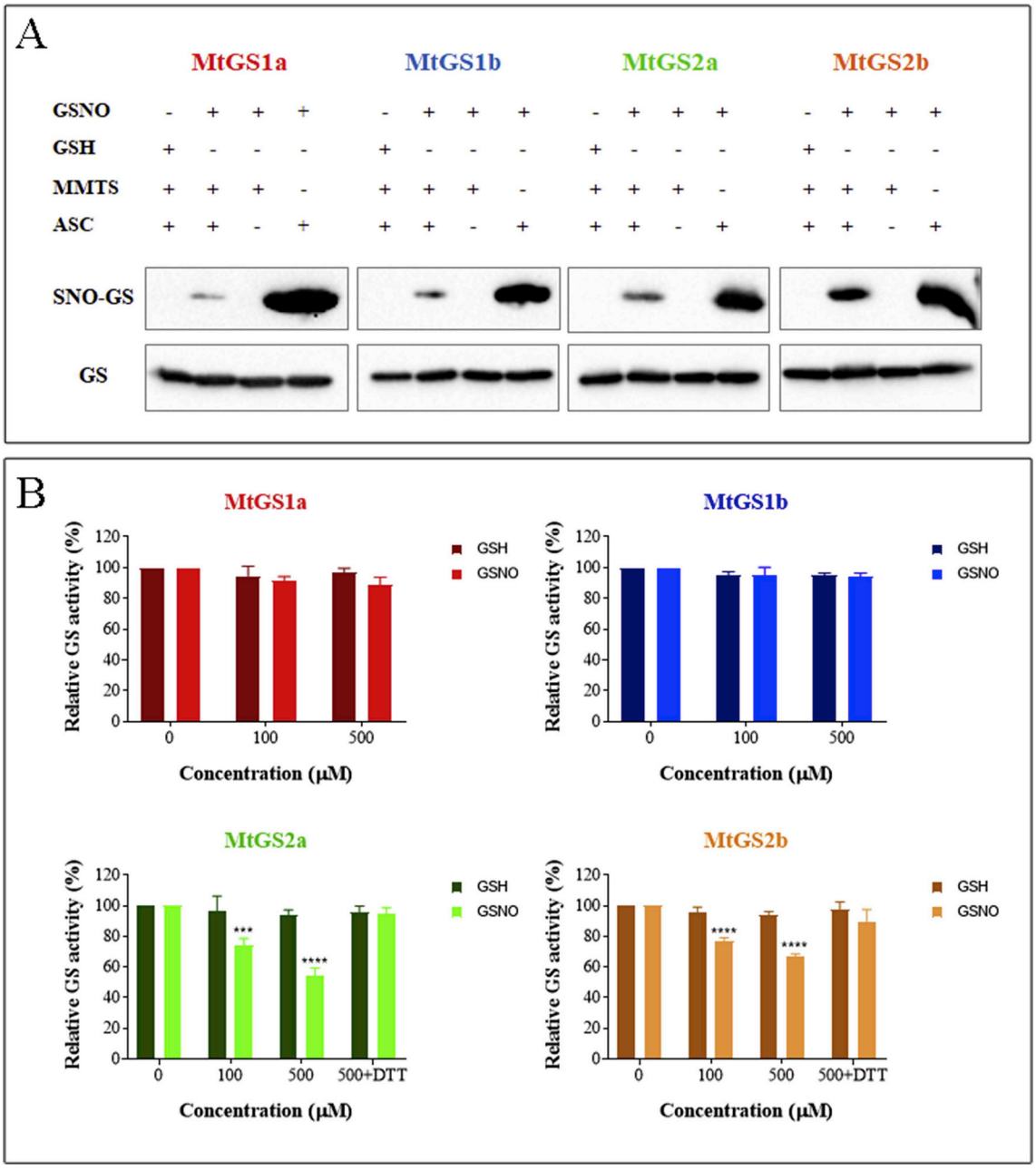

Fig. 1. *In vitro* analysis of *S*-nitrosation of each individual *M. truncatula* GS isoenzyme. A - Analysis of GS *S*-nitrosation using the biotin-switch technique. Ten μg of recombinant MtGS1a, MtGS1b, MtGS2a or MtGS2b were incubated with 500 μM GSNO or 500 μM GSH and subjected to the biotin-switch assay. Biotinylated proteins were purified by avidin-affinity chromatography, separated by SDS-PAGE and visualized by Western blot using an anti-GLN1|GLN2 antibody (Agrisera) (SNO-GS). The addition (+) or omission (−) of GSH, GSNO, MMTS or ascorbate (ASC) during the assay is indicated. Loading controls were obtained by immunoblot detection of GS before avidin-affinity chromatography (GS). This result is representative of two independent experiments. **B** - Evaluation of the effect of GSNO on GS activity. Each purified recombinant GS isoenzyme (MtGS1a, MtGS1b, MtGS2a or MtGS2b) was incubated with GSH or GSNO at increasing concentrations and assayed for GS activity. MtGS2a and MtGS2b were additionally treated with 500 μM GSNO, followed by incubation with 10 mM DTT, and assayed for GS activity. GS activity was normalized to that found in the absence of chemical reagents and is represented as means ± SD of at least 4 independent experiments assayed in duplicate. The average initial GS activities were 413, 296, 251 and 12 μmol min^{-1} mg $protein^{-1}$ for MtGS1a, MtGS1b, MtGS2a and MtGS2b, respectively. Asterisks indicate significant differences from the GSH-treated samples (***$p < 0.001$,****$p < 0.0001$, Student's t-test).

Cys304 appears to be important for GS activity, it is not relevant for the GSNO-induced inactivation. However, we cannot exclude the existence of additional cysteine residues important for the inactivation process or the contribution of other oxidative modifications induced by NO, as the mutated protein was still susceptible to inhibition by GSNO, although to a much lower extent.

The three mutated proteins were also subjected to a biotin-switch analysis, but surprisingly all, including the double mutant MtGS2aC304S/C369S could still be detected as *S*-nitrosated following BST (Fig. 3), indicating the existence of additional *S*-nitrosation sites in cysteines that are common to the cytosolic GSs. We, therefore, proceeded to the identification of the *S*-nitrosated residues in both the cytosolic and plastid located enzymes by mass spectrometry.

3.3. Mass spectrometry identification of S-nitrosated cysteines in cytosolic and plastid located GSs

Purified MtGS1a and MtGS2a were *in vitro* *S*-nitrosated and

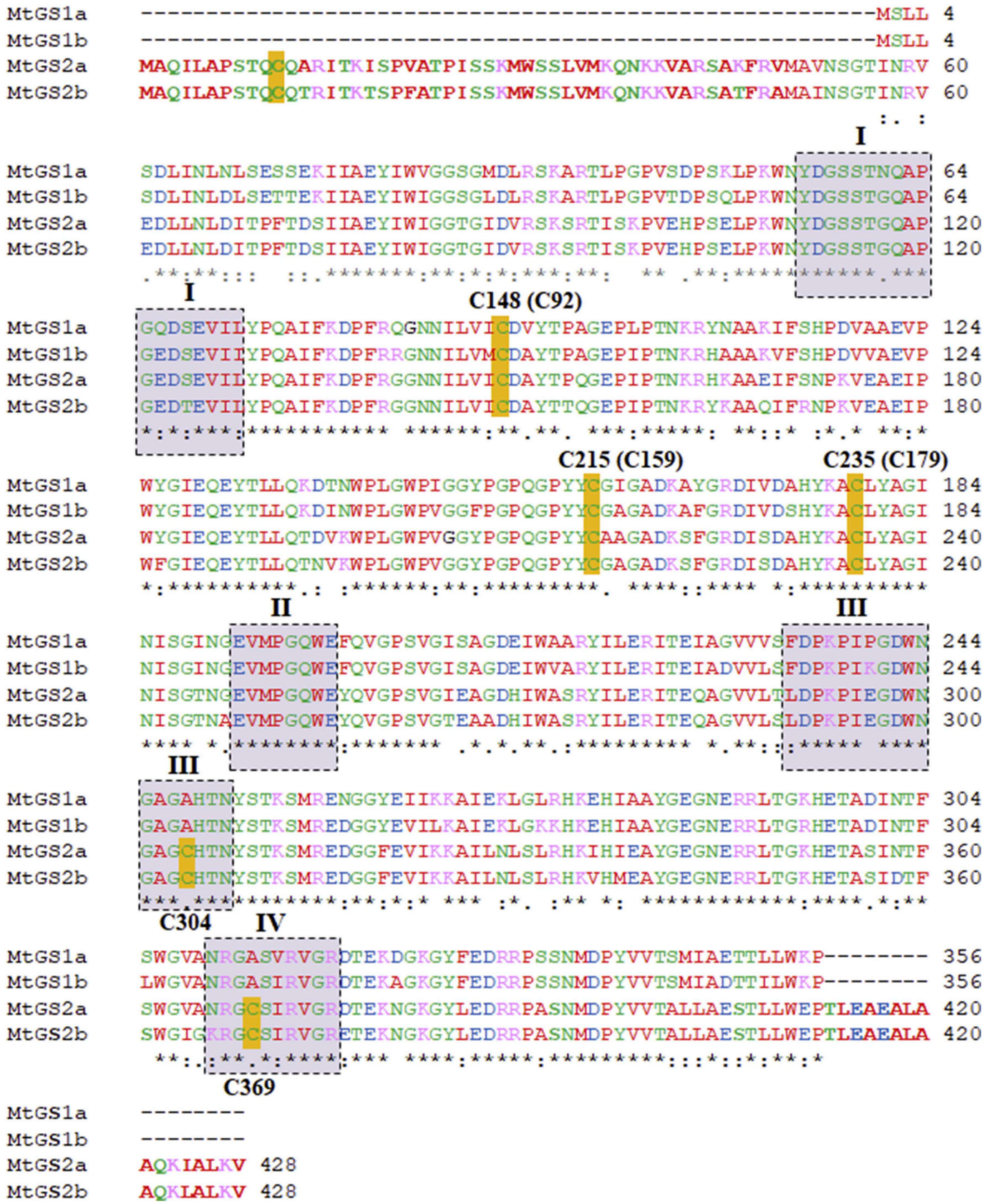

Fig. 2. Alignment of the amino acid sequences of the four MtGS isoenzymes. The cysteine residues are highlighted in yellow and the five cysteine residues present in the mature form of MtGS2a are numbered. The position of the three cysteine residues in MtGS1a is shown between brackets. The GS conserved regions I to IV, defined by Eisenberg et al. [51], are also indicated. The MtGS2a and MtGS2b transit peptides and C-terminal extension characteristics of plastid-located GS are shown in boldface. Residues are colored according to their physicochemical properties as follows: AVFPMILW in red, DE in blue, RK in magenta, and STYHCNGQ in green. (*) residues fully conserved; () highly conserved; (.) poorly conserved and () not conserved.

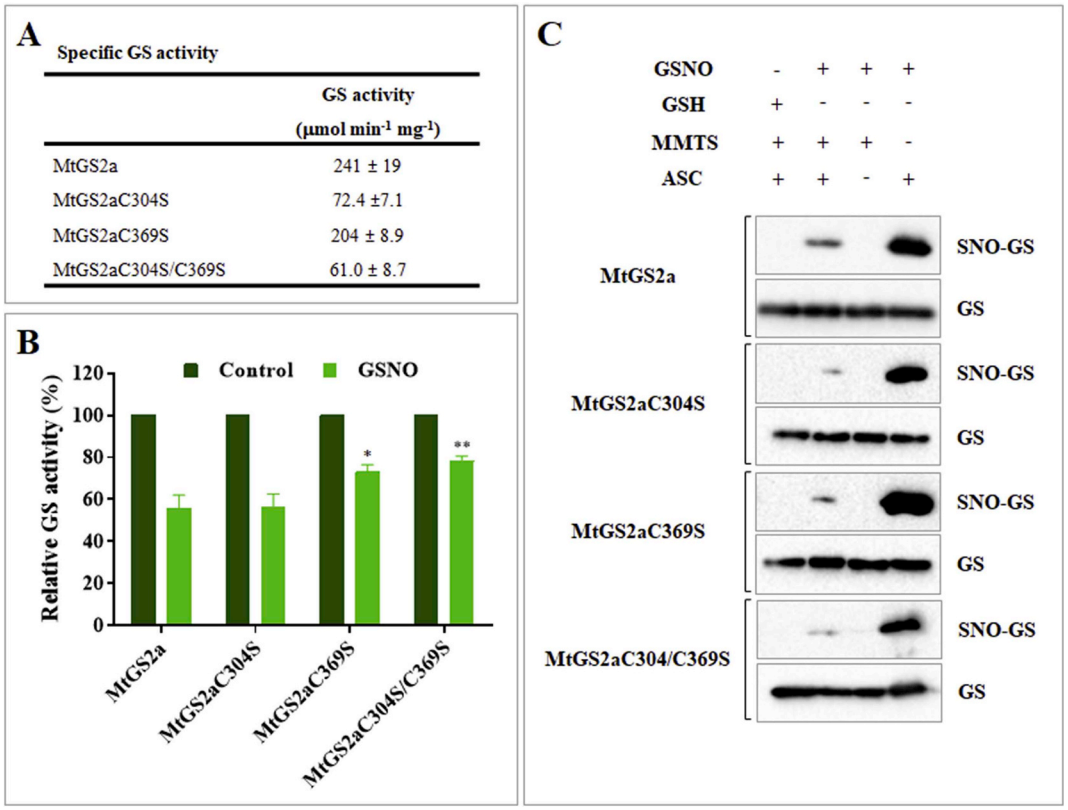

Fig. 3. Evaluation of the relevance of Cys304 and Cys369 for MtGS2a inactivation by *S*-nitrosation. **A** - Specific GS activity of purified MtGS2a, MtGS2aC304S, MtGS2aC369S, and MtGS2aC304S/C369S. The values represent the average ± SD of at least three independent determinations. **B** - Effect of *S*-nitrosation on the activity of MtGS2a, MtGS2aC304S, MtGS2aC369S, and MtGS2aC304S/C369S. Purified enzymes were incubated with 500 μM GSNO and assayed for GS transferase activity. GS activity was normalized to that found in the absence of reagents and is represented as means ± SD of at least 3 independent experiments, assayed in duplicated. Asterisks indicate significant differences relative to the activity of GSNO-treated MtGS2a (*$p < 0.05$, **$p < 0.01$, Student's t-test). **C** - Biotin-switch of MtGS2a, MtGS2aC304S, MtGS2aC369S, and MtGS2aC304S/C369S treated with 500 μM GSNO. After BST, biotinylated proteins, purified by avidin-affinity chromatography, were analyzed by Western blot using anti-GLN1|GLN2 antibody (Agrisera) (SNO-GS). The addition (+) or omission (−) of GSH, GSNO, MMTS or ASC during the assay is indicated. Loading controls were obtained by immunoblot detection of GS before avidin-affinity chromatography (GS). The results are representative of two independent experiments.

analyzed by nLC-MS/MS. Because the SNO group is naturally unstable, the *S*-nitrosated proteins were subjected to the BST prior to the mass spectrometry analysis in order to replace the SNO groups by biotin. After biotin-HPDP labeling, the proteins were subjected to trypsin digestion, under non-reducing conditions, and the resulting peptides were analyzed by nLC-MS/MS. To enable a direct comparison of tryptic peptides and simplify the identification of modified peptides the non-nitrosated MtGS1a and MtGS2a (GSH-treated) were analyzed in parallel. The expected and observed monoisotopic masses ($[M+H]^+$) of the tryptic peptides containing cysteine residues either unmodified, MMTS alkylated (+methylthio) or modified with biotin-HPDP are presented in Tables 1 and 2.

The analysis of GSNO-treated MtGS1a by nLC-MS/MS following biotin-switch and digestion with trypsin led to the detection of multi-charged peptides harboring Cys92 (*m/z* 28884.443 and *m/z* 3040.539) or Cys159 (*m/z* 3854.785) modified with biotin-HPDP (Table 1) identifying both residues as *S*-nitrosation targets in MtGS1a. However, the peptides harboring Cys92 or Cys159 were also detected as MMTS alkylated, which indicates that the proteins were only partially *S*-nitrosated. Cys92 was further detected in the unmodified form. Since the biotin-HPDP labeling follows the ascorbate-specific reduction of *S*-nitrosothiols, the detection of an unmodified cysteine indicates that it was *S*-nitrosated in the starting sample but the labeling reaction of the nascent thiol during the biotin-switch assay was incomplete. Detection of unmodified cysteine residues could indicate inefficient alkylation and/or biotin-HPDP labeling. However, peptides containing unmodified cysteines were not detected in the GSH-treated samples (data not shown), indicating that all the reduced cysteine residues have been effectively blocked by iodoacetamide.

Regarding MtGS2a, the nLC MS/MS analysis of the GSNO-treated protein identified tryptic peptides harboring Cys148 (*m/z* 2998.498) and Cys304 (*m/z* 3842.864) modified with biotin-HPDP but also alkylated with MMTS (Table 2). Surprisingly, the tryptic peptide containing Cys369 previously shown to be *S*-nitrosated was not detected either biotinylated or MMTS alkylated. However, its detection in the unmodified form (*m/z* 2705.358), indicates that this residue was initially *S*-nitrosated, otherwise it should have been detected as MMTS alkylated. This finding is further supported by a MALDI-TOF/TOF analysis of GSNO-treated MtGS2a, which clearly identified Cys369 as an *S*-nitrosated residue. A peptide of *m/z* 963.474 in good agreement with the expected *m/z* value of a Cys369 harboring peptide (^{368}G<u>C</u>SIR^{372}) modified with biotin-HPDP (mass increase of 428.61) was detected in GSNO-treated MtGS2a but not in the GSH-treated protein (Table 3), but the MALDI-TOF/TOF analysis failed to detect the other S-nitrosated residues, which were clearly identified by nLC MS/MS. This reflects the different sensitivity of the two techniques and is a good example of the technical difficulties associated with the detection of specific peptides by mass spectrometry.

Taken together, the results obtained by the combination of the two techniques indicate that MtGS1a and MtGS2a share one *S*-nitrosation site at a conserved cysteine (Cys92 in MtGS1a, corresponding to Cys148 in MtGS2a) and MtGS2a contains two additional *S*-nitrosation sites (Cys304 and Cys369) corresponding to the two cysteine residues exclusive of the plastid-located enzymes.

Table 1
Determination of modified cysteine residues in MtGS1a by nLC-MS/MS.

Modifications $[M+H]^+$	+ biotin-HPDP *m/z*	2884.441/2884.443	3407.569/nd	4691.255/nd	
	Expected/Observed	3040.542/3040.537	3854.792/3854.803		
		3555.791/nd	4796.252/nd		
	+ Methylthio *m/z*	2502.237/2502.234	3025.365/3025.368	4309.051/4309.067	
	Expected/Observed	2658.338/2658.344	3472.588/3472.596		
		3173.587/3173.590	4414.048/4414.060		
	Unmodified *m/z*	2456.247/nd	2979.377/nd	4263.063/nd	
	Expected/Observed	2612.350/2612.369	3426.598/nd		
		3127.597/nd	4368.058/nd		
Sequence		^{84}QGNNILVI**C**DVYTPAGEPLPTNK^{106}	^{138}DTNWPLGWPIGGYPGPQGPYY**C**GIGADK^{165}	^{178}A**C**LYAGINISGINGEVMPGQWEFQVGPSVGISAGDEIWAAR^{218}	
		^{84}QGNNILVI**C**DVYTPAGEPLPTNKR^{107}	^{138}DTNWPLGWPIGGYPGPQGPYY**C**GIGADKAYGR^{169}		
		^{80}DPFRQGNNILVI**C**DVYTPAGEPLPTNKR^{107}	^{138}DTNWPLGWPIGGYPGPQGPYY**C**GIGADKAYGRDIVDAHYK^{177}		

Purified MtGS1a was treated with 500 μM GSNO and assayed by BST in order to replace the SNO group by biotin. After tryptic digestion under non-reducing conditions, the Cys-containing peptides were analyzed for modifications with MMTS (+Methylthio) or biotin-HPDP by mass spectrometry. The expected and observed m/z values for each peptide detected are shown. The values reported correspond to the mass of the most abundant isotope. nd – not detected.

Table 2
Determination of modified cysteine residues in MtGS2a by nLC-MS/MS.

Modifications	+ biotin-HPDP *m/z*	3513.744/nd	4412.052/nd	4761.236/nd	3842.855/3842.864	3133.968/nd
$(M + H)^+$	Expected/Observed	3357.643/nd	3482.627/nd			
		2998.495/2998.498	3035.404/nd			
		2842.394/nd				
	+ Methylthio *m/z*	3131.540/3131.543	4029.848/4029.854	4379.032/4379.033	3460.651/3460.664	2751.348/nd
	Expected/Observed	2975.439/2975.442	3100.423/3100.431			
		2616.291/2616.293	2653.200/2653.199			
		2460.190/2460.193				
	Unmodified *m/z*	3085.550/nd	3983.858/nd	4333.042/nd	3414.663/3414.666	2705.358/2705.358
	Expected/Observed	2929.449/nd	3054.433/nd			
		2570.301/nd	2607.210/nd			
		2414.200/nd				
Sequence		^{136}DPFRGGNNILVI**C**DAYTPQGEPIPTNKR^{163}	^{197}WPLGWPVGGYPGPQGPYY**C**AAGADKSFGRDISDAHYK^{233}	^{234}A**C**LYAGINISGTNGEVMPGQ-WEYQVGPSVGIEAGDHIWASR^{274}	^{280}ITEQAGVVLTLDPKPIE-GDWNGAG**C**HTNYSTK^{311}	^{348}LTGKHETASINTFS-WGVANRG**C**SIR^{372}
		^{136}DPFRGGNNILVI**C**DAYTPQGEPIPTNK^{162}	^{197}WPLGWPVGGYPGPQGPYY**C**AAGADKSFGR^{225}			
		^{140}GGNNILVI**C**DAYTPQGEPIPTNKR^{161}	^{197}WPLGWPVGGYPGPQGPYY**C**AAGADK^{221}			
		^{140}GGNNILVI**C**DAYTPQGEPIPTNK^{162}				

Purified MtGS2a was treated with 500 μM GSNO and assayed by BST in order to replace SNO group by biotin. After tryptic digestion under non-reducing conditions, the Cys-containing peptides were analyzed for modifications with MMTS (+Methylthio) or biotin-HPDP by mass spectrometry. The expected and observed m/z values for each peptide detected are shown. The values reported correspond to the mass of the most abundant isotope nd – not detected.

Table 3
Determination of modified cysteine residues in MtGS2a by MALDI-TOF/TOF.

Modifications						
(M + H)$^+$	+ biotin-HPDP *m/z*	3513.155/nd	3034.813/nd	4761.654/nd	3842.266/nd	963.876/963.474
	Expected/Observed	2841.803/nd	3482.038/nd			
		2997.906/nd				
	+ Methylthio *m/z*	3130.533/3131.537	2652.193/2653.199	4378.025/4379.022	3459.644/3460.664	581.256/nd
	Expected/Observed	2459.183/2460.189	3099.416/3100.419			
		2615.284/2616.286				
	Unmodified *m/z*	3084.545/nd	2606.203/nd	4333.044/nd	3413.656/nd	535.266/535.249
	Expected/Observed	2413.193/nd	3053.428/nd			
		2569.296/nd				
Sequence		^{136}DPFRGGNNILVICDAYTPQGEPIPTNKR^{163}	^{197}WPLGWPVGGYPGPQGPYYCAAGADK^{221}	^{234}ACLYAGINISGTNGEVMPGQWEYQVG-PSVGIEAGDHIWASR^{274}	^{280}TTEQAGVVLTLDPKPIEGDWN-GAGCHTNYSTK^{311}	^{368}GCSIR^{372}
		^{140}GGNNILVICDAYTPQGEPIPTNK^{162}	^{197}WPLGWPVGGYPGPQGPYYCAAGADKSFGR^{225}			
		^{140}GGNNILVICDAYTPQGEPIPTNKR^{163}				

Purified MtGS2a was treated with 500 μM GSNO and assayed by BST in order to replace SNO group by biotin. After trypsin digestion under non-reducing conditions the tryptic peptides were analyzed for modifications with MMTS (+methylthio) or biotin-HPDP by MALDI-TOF/TOF MS. The expected and observed m/z values for each Cys containing peptide detected are shown. The theoretical masses were obtained using the PeptideMass program (considering all Cys in reduced form and non-oxidized methionines. The masses of the identified peptides were determined by MALDI-TOF/TOF analysis being the spectra calibrated with the trypsin peptides. nd – not detected.

3.4. Analysis of the position of the S-nitrosated residues within the three-dimensional structure of the proteins

The three-dimensional structure of MtGS1a has been previously solved at a 2.23 Å resolution by X-ray crystallography [50] it is thus possible to know the precise location of the cysteine residues within the quaternary structure of the proteins and enlighten the structural basis of the regulation of GS by *S*-nitrosation. Plant GS is a decameric enzyme, composed by two superposed pentameric rings, and the active sites are formed at the interface between two neighboring subunits, in a funnel-shaped cavity. The amino acids directly interacting with the enzyme's substrates derive from the N-terminal domain of one subunit and the C-terminal domain of the other, in a total of 10 active sites per molecule. This active-site structure is well conserved between all GS proteins among all life kingdoms. MtGS1a contains only three cysteine residues, and none of them is directly involved in substrate binding. The position of the three cysteines within the three-dimensional structure of MtGS1a is shown for one of the monomers of the decameric protein in the structural overview presented in Fig. 4A. A detailed view of the interface between two neighboring subunits reveals that Cys92 is located in a β-sheet motif located at the N-terminal domain of the subunit represented in blue, Cys159 in a loop that protrudes into the funnel-shaped cavity that forms the active site, and Cys179 is positioned in a buried α-helix at the C-terminal domain (Fig. 4 B). The two MtGS1a identified *S*-nitrosation sites, Cys92 and Cys159, are found on the surface of the enzyme, partially or completely exposed to the solvent. The third MtGS1a cysteine residue, Cys179, is positioned in a buried α-helix, its reduced accessibility explains why it was not detected as an *S*-nitrosation site.

MtGS1a and MtGS2a share a high percentage of amino acid identity, a similar decameric arrangement and active site fold, as shown in Torreira et al. [50]. Therefore, we used the three-dimensional structure of MtGS1a as template to model the conformation of MtGS2a and predict the position of the two unique cysteine residues within the three-dimensional structure of the protein (Fig. 4C). According to this model, the two cysteine residues exclusive of the plastid-located enzymes (Cys304 and Cys369), are positioned inside the active site cavity and therefore are likely relevant for the catalytic properties of the proteins. However, Cys369 (Ala313 in MtGS1a) is closer to the active site entrance than Cys304 (Ala248 in MtGS1a). The location of Cys304 in a deeper position within the active site cavity explains why the specific activity of the enzyme is reduced when Cys304 is mutated to serine. However, this residue was found to be irrelevant for the GSNO-induced inactivation and the important residue for the regulatory effects of *S*-nitrosation on MtGS2a is Cys369. Consistently, the analysis of the structural environment of Cys369 (Ala313 in MtGS1a) shows that the residue is located in one of the walls of the funnel shaped cavity, in a region rich in polar residues and strictly conserved, with notable exposition of the cysteine residue. It is thus conceivable that upon *S*-nitrosation, new polar interactions are established altering the conformation of this crucial regulatory region in the neighborhood of the enzyme active site, resulting in enzyme inactivation.

3.5. Analysis of GS S-nitrosation in planta

To evaluate whether GS is *S*-nitrosated *in planta*, the endogenous *S*-nitrosated proteins were isolated from leaves and root nodules of *M. truncatula* via the biotin-switch assay. The resulting biotinylated proteins were purified by avidin-affinity chromatography and analyzed by Western blot (Fig. 5). The detection of an immunoreactive GS polypeptide of 42 kDa, compatible in size with the plastid located GS, in leaf and nodule extracts shows that GS2 is endogenously *S*-nitrosated in both organs (Fig. 5). In root nodules, in addition to the 42 kDa GS polypeptide, a more abundant GS polypeptide of 39 kDa is clearly detected, indicating that both the plastid and cytosolic enzymes are *S*-nitrosated in root nodules of *M. truncatula* (Fig. 5B). The *S*-nitrosated

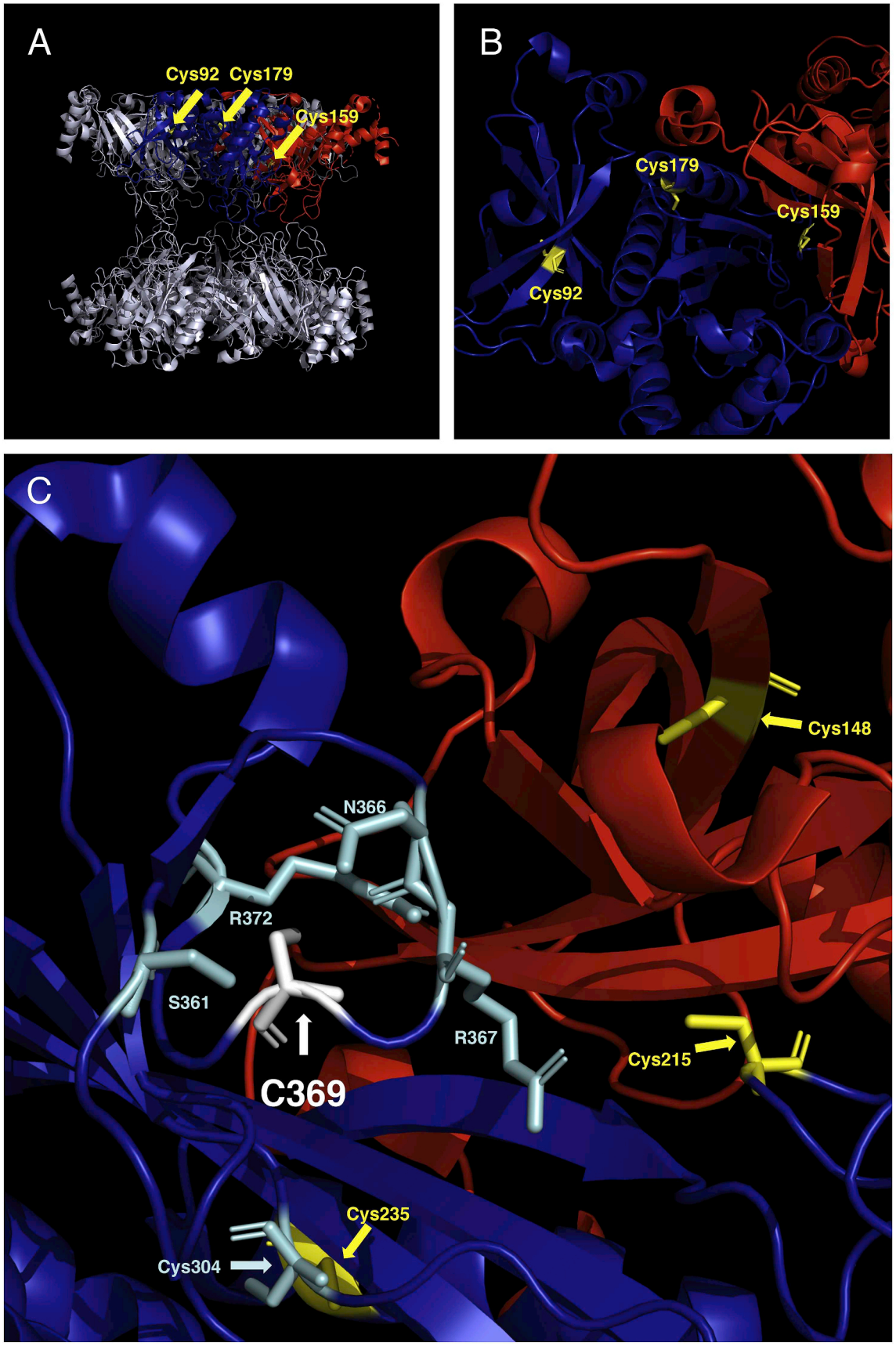

(caption on next page)

Fig. 4. Location of the regulatory *S*-nitrosation sites within the three-dimensional structure of GS. **A** - Side-view of the three-dimensional structure of the MtGS1a decamer as determined by Torreira et al. [50], with the subunits A and E highlighted in blue and red, respectively. The localization of cysteines 92, 159 and 179 within subunit A are shown in yellow and pointed out with arrows. **B** - Expanded view of the position of the three MtGS1a cysteine residues within subunit A. **C** – View of the conserved GS active site showing the position of the five MtGS2a cysteine residues. The figure represents the active site of MtGS1a, in which the position of the unique MtGS2a cysteine residues within the protein folded structure is projected by replacing the MtGS1a residues Ala248 and Ala313 by the corresponding cysteine residues in MtGS2a: Cys304 (shown in cyan) and Cys369, (shown and white). Cysteines common to MtGS1a are labeled in yellow (Cys148, Cys215, and Cys235). The predicted position of Cys369 in one of the walls of the funnel-shaped cavity that forms the conserved GS active site is highlighted. The neighboring amino acids identified in the figure are conserved in the two classes of proteins: S361 (corresponding to S305 in MtGS1a), N366 (corresponding to N310 in MtGS1a), R367 (corresponding to R311 in MtGS1a) and R372 (corresponding to R316 in MtGS1a).

cytosolic GS detected in root nodules most probably correspond to MtGS1a, as it is the main cytosolic isoenzyme expressed in nodules, where it functions to assimilate the ammonium that is abundantly produced by bacterial N fixation. The inclusion of both negative and positive controls performed without addition of ascorbate or MMTS, respectively, ensures the specificity of the technique. When ascorbate is omitted GS is not detected confirming that the GS signal observed is ascorbate-dependent and does not result from a possible non-selective photo-inducible biotinylation by biotin-HPDP or from endogenous biotinylation of GS proteins (Fig. 5A and B, second lane). Conversely, the omission of MMTS leads to a strong GS signal due to the biotinylation of several cysteine residues confirming the efficiency of MMTS as blocking agent (Fig. 5A and B, third lane). The total GS polypeptide content in the leaf and nodule extracts used for the biotin-switch assay is also presented in Fig. 5 to show the relative GS polypeptide content in the initial extracts (Fig. 5A and B – Total GS). These results demonstrate that both MtGS1a and MtGS2a are *S*-nitrosated *in planta* under physiological conditions, thus suggesting that the regulation of GS by *S*-nitrosation is probably physiologically relevant within the leaf and root nodule contexts.

4. Discussion

Nitric oxide regulates multiple physiological processes in plants by the induction of precisely targeted covalent post-translational modifications on specific proteins. Thus, the identification of its direct targets and the characterization of the molecular details and physiological effects of the NO-induced modifications on target proteins are essential to understand NO bioactivity. Here, we show that the key nitrogen metabolic enzyme glutamine synthetase is a *S*-nitrosation target in *M. truncatula* and we demonstrate that *S*-nitrosation differentially affects the activity of the two major classes of GS isoenzymes.

GS is a very interesting target for *S*-nitrosation because the enzyme occupies a central position in N metabolism and as NO production is necessarily closely linked to N metabolism, the enzyme may play an important role at the crossroads of signaling events, linking NO signaling with NO production and N metabolism. Interestingly, an interconnection between N assimilation and NO signaling, through *S*-nitrosation, has recently been disclosed. It has been shown that NO controls its own bioavailability, by controlling its generation via nitrate assimilation and its scavenging via the enzyme GSNO reductase (GSNOR) [41]. Given that the levels of GSNO are controlled by the enzyme GSNOR, which catalyzes the reduction of GSNO to oxidized glutathione (GSSG) and ammonium, and GS is the plant enzyme responsible for the reassimilation of ammonium, the finding that GS, similarly to GSNOR, is regulated by *S*-nitrosation inserts an additional player in this complex network of signal exchanges.

GS is a highly complex and highly regulated enzyme, existing as a number of isoenzymes with specific kinetic properties and specific mechanisms of post-translational regulation. It is interesting that although all the *M. truncatula* GS isoenzymes are susceptible to *S*-nitrosation, only the activity of plastid-located isoenzymes is affected by this redox-based modification. The activity of the *M. truncatula* cytosolic enzymes is also highly affected by NO, but through a different post-translational mechanism, tyrosine nitration [20]. The finding that isoenzymes sharing a high degree of sequence homology and a highly conserved active site fold are differentially modified by NO reflects the specificity of each of the NO-induced PTMs and illustrates the complexity and sophistication of the post-translational mechanisms operating to regulate GS activity.

The identification of the exact sites of *S*-nitrosation can provide valuable insights into the molecular mechanisms underlying the structural alterations induced in target proteins. The mass spectrometry analysis of MtGS1a and MtGS2a identified multiple *S*-nitrosation sites in both proteins. One of the *S*-nitrosated cysteines is common to the cytosolic and plastid-located enzymes, reflecting the structural

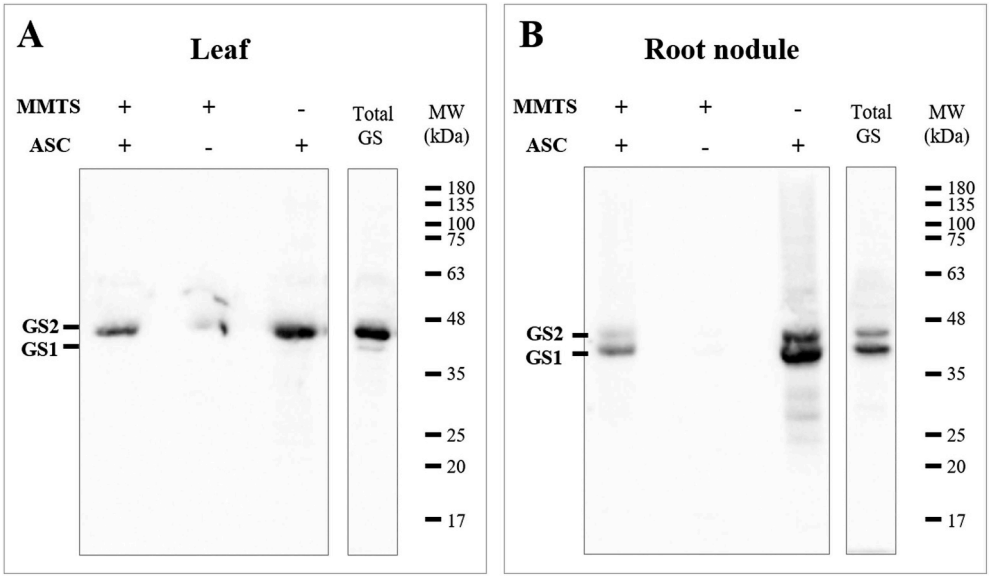

Fig. 5. Evaluation of GS *S*-nitrosation in leaves and root nodules of *M. truncatula*. Soluble proteins extracted from *M. truncatula* leaves (**A**) or root nodules (**B**) were subjected to the biotin switch assay. After purification by avidin affinity chromatography, the endogenously *S*-nitrosated proteins were separated by SDS-PAGE and immunoblotted using an anti-GLN1|GLN2 antibody, which recognizes both GS1 and GS2 polypeptides. Addition (+) or omission (−) of the reaction components ascorbate (ASC) and MMTS during the assay is indicated in the upper panel. The GS polypeptide content in the initial extracts is also shown (total GS). The results are representative of three independent experiments.

similarities between the two proteins [50]. MtGS2a contains two additional cysteines and both are susceptible to *S*-nitrosation, however, only the substitution of Cys369 results in a significant reduction in the GSNO-mediated inhibitory effect, thus indicating that it is the relevant *S*-nitrosation regulatory site. An analysis of the structural environment of Cys369 revealed that it is located in a region rich in polar residues, in one of the walls that forms the active site and at an accessible position. Thus, the mechanism of MtGS2a inactivation by *S*-nitrosation can be elucidated in structural terms as *S*-nitrosation of Cys369 may lead to new polar interactions, altering the conformation of a crucial region in the neighborhood of the enzyme active site, resulting in enzyme inactivation. It is remarkable that Cys369 is absolutely conserved in all plant GS2 proteins, integrating one of the conserved catalytic regions defined by Eisenberg et al. [51] and, together with Cys304, appear to be important for the redox regulation of the plastid-located enzymes [32,52]. Here, we show that Cys369 and not Cys304 is the relevant *S*-nitrosation site for the regulation of MtGS2a activity. It is expectable that S-nitrosation totally inhibits the catalytic activity, but the mass spectrometry analysis revealed that the proteins were only partially *S*-nitrosated under our experimental conditions suggesting that the inhibitory effect of *S*-nitrosation on MtGS2a is probably more effective than observed and that eventual consequences on the activity of MtGS1a could have been missed. However, the analysis of the structural environment of the *S*-nitrosated residues in MtGS1a, suggests that potential alterations in protein conformation induced by the addition of the NO group to Cys92 or Cys159 unlikely interfere with the enzyme's catalytic activity. Still, we cannot discard a possible indirect effect, for example by inducing conformational changes that could result in the creation of a binding site for interaction with other proteins. It is noteworthy that all the cysteine residues of cytosolic GS are highly conserved among all eukaryotes, including plants, animals and humans. In animals, GS is extremely important, especially in the brain where its activity is vital for the detoxification of the highly toxic ammonia, indeed defects in GS activity are frequently associated with neurodegenerative disorders [53]. Interestingly, it has been reported that GS is also prone to S-nitrosation in mammals, but little is known regarding its functional effects [54,55]. The studies on S-nitrosation of the well-conserved cysteine residues of plant GS here reported can be useful to enlighten the NO-mediated regulation of GS in animals.

Despite the great advantage of using recombinant proteins to independently analyze the modifications occurring in individual GS isoenzymes, *in vitro* studies involving highly reactive chemical reagents are prone to artifacts. The characterization of the specific NO-mediated PTMs occurring *in planta* is therefore required to understand the physiological relevance of the regulation of GS by NO. Using the biotin-switch assay, we demonstrate that both the cytosolic and the plastid-located GSs are *S*-nitrosated *in planta*, revealing that a steady-state level of *S*-nitrosated GS exists *in vivo,* both in leaves and root nodules. This may reflect a need for an abundant source of readily available protein that could be easily denitrosated in case of ammonium accumulation to dangerous levels, this at least for MtGS2a where *S*-nitrosation inhibits enzyme activity. Cytosolic and plastid-located GS isoenzymes have been previously identified as potential *S*-nitrosation targets by distinct biotin-switch based proteomic approaches [8,16,56]. However, these approaches always include a pre-treatment with an exogenous NO donor to increase the probability of detecting *S*-nitrosated proteins, which is an artificial setup that does not reflect the *S*-nitrosation status under normal physiological conditions. Here we show, for the first time, that both cytosolic and plastid-located GSs are *S*-nitrosated within a natural physiological context.

We found that both the cytosolic and plastid-located GSs are among the *S*-nitrosated proteins in *M. truncatula* root nodules. The regulation of GS in root nodules is of major interest due to the key location of this enzyme in the pathways between the nitrogen-fixing bacteria and the plant and the importance of legumes in the global nitrogen cycle and agricultural systems. Both MtGS1a and MtGS2a are expressed in the root nodule infected cells, in which NO is abundant [57,58], the enzymes are thus accessible to be modified by NO. We have previously shown that MtGS1a is regulated by tyrosine nitration in root nodules and that its nitration status is inversely correlated with active N fixation [20]. Nitration of MtGS1a causes total enzyme inactivation and the finding that it is also subjected to *S*-nitrosation suggests that the enzyme is subjected to a dual mechanism of regulation by NO, in a comparable manner to what has been shown for pea ascorbate peroxidase, whose activity is inhibited by tyrosine nitration and enhanced by *S*-nitrosation [14]. The impact of the two NO-induced modifications on MtGS1a activity is also quite different, tyrosine nitration completely inactivates the enzyme, but *S*-nitrosation does not seem to directly impact MtGS1a activity. Interestingly, the MtGS1a regulatory nitration site (Tyr 167) [20] is located in close vicinity to one of the identified *S*-nitrosated cysteines (Cys159), and both are located close to the catalytic center. It is tempting to speculate that the modification of Cys159 by *S*-nitrosation could drive changes in the quaternary structure affecting nitration of Tyr 167. This way, GS inhibition by tyrosine nitration could be directly regulated by *S*-nitrosation, which in turn, could be regulated by the type of NO-radicals available within certain physiological contexts. Future work should focus on the regulatory significance of the dual mechanism of regulation of MtGS1a by NO-derived molecules, both by Tyr nitration and *S*-nitrosation and on the physiological relevance of these regulatory mechanisms for root nodule functioning.

Here, we demonstrate that the activity of the plastid located GS is directly affected by S-nitrosation and we show that the enzyme is S-nitrosated in the leaves, supporting a physiological meaning for the regulation of GS2 by NO. To uncover the biological role of GS2 S-nitrosation is however a challenging task because on one hand, the enzyme is regulated at multiple levels and is involved in different metabolic pathways, and on the other hand the origins and sites of NO production as well as the type of NO radical formed at each site are still far from being elucidated. It has been demonstrated that NO biosynthesis in plants relies on nitrite and L-arginine dependent pathways, and can occur in cytosol, chloroplasts, mitochondria, and peroxisomes, but it is also known that NO can readily diffuse within the cell [59,60]. Despite the controversy around NO synthesis in plants, it is consensual that nitrate reductase (NR) represents a major enzymatic source of NO production in plant cells. In addition to its main anabolic function in nitrate assimilation, NR can act as nitrite:NO reductase resulting in the formation of nitric oxide (NO). Interestingly, MtGS2a is the isoenzyme responsible for the assimilation of the ammonium derived from nitrate reduction, which involves an additional enzyme, nitrite reductase (NiR) located in the plastid. Thus GS2 is metabolically linked to NR. As it is known that the activity of NR in the production of NO is dependent on nitrite accumulation [60], it is tempting to speculate that the regulation of GS2 by S-nitrosation could be related to NO production via NR. Under increased nitrite concentrations in the cytosol, NR functions as an NO producing enzyme, increasing NO concentration, which could diffuse to the plastid and ultimately result in the reversible inhibition of GS2 activity through S-nitrosation, thus shutting-down temporarily the assimilation of nitrate-derived ammonium. This could be important under conditions in which carbon fixation rates are low and nitrogen availability is high, providing a mechanism to block nitrogen assimilation to maintain the carbon to nitrogen ratio.

Another crucial function of plastid GS is the reassimilation of the ammonium released during photorespiration, and S-nitrosation of GS2 could also represent a regulatory mechanism to fine-tune plastid-located GS activity to the photorespiration rates. Interestingly, the majority of SNO targets in the leaves are associated with the chloroplast [16,61], what is not surprising because photosynthesis is an impressive source of reactive oxygen species and the redox regulation of protein function is of great importance in chloroplasts. In recent years, protein *S*-nitrosation has been established as a broad-based mechanism for the post-translational regulation of many proteins involved in photosynthesis and photorespiration [62,63]. In fact, *S*-nitrosated proteins cover

nine of the fourteen steps in the Calvin-Benson cycle in *Arabidopsis thaliana* [16] and several enzymes involved in photorespiration have also been identified as targets of NO-dependent PTMs, suggesting that NO may also regulate this metabolic pathway [63]. Considering that the main effect of *S*-nitrosation on metabolic enzymes is activity inhibition, as we observed for MtGS2a, it is conceivable that *S*-nitrosylation could represent a molecular switch to turn off enzyme activities during the night, regulating both photosynthesis and photorespiration. Whether the regulation of GS2 activity by S-nitrosation is related to photorespiration, nitrate assimilation, or both requires further research. It would be important to investigate if the MtGS2a S-nitrosation status changes during the diurnal cycle or in response to increase nitrite levels.

In conclusion, this study identifies all the members of the *M. truncatula* GS family as targets of *S*-nitrosation and reveals interesting differences between the regulatory effects of GNO on specific GS isoenzymes. It is still unclear what could be the biological role of GS *S*-nitrosation *in planta*, but here we show that endogenous *S*-nitrosation of both the cytosolic and plastid-located GSs occurs under physiological conditions supporting a biological meaning for S-nitrosation. It is remarkable that isoenzymes sharing a high degree of sequence homology and a highly conserved active site fold can be differentially modified by *S*-nitrosation, strengthening the idea that the NO signaling effects are specific under defined physiological contexts. In addition to a differential susceptibility of individual GS isoenzymes to NO, the differential localization of specific isoenzymes in a particular plant tissue and subcellular compartment, is likely to be implied in the NO-mediated regulation of GS activity.

Acknowledgments

We gratefully acknowledge Pedro Pereira (i3S – Institute for Health Research and Innovation, Porto, Portugal) for the help on the structural analysis of GS proteins and Hugo Osório (Proteomics Platform at i3S – Institute for Health Research and Innovation, Porto, Portugal) for the proteomics analysis and valuable suggestions and discussions.

Appendix A. Supplementary data

Supplementary data to this article can be found online at https://doi.org/10.1016/j.niox.2019.04.006.

Funding

This research was supported by the Fundo Europeu de Desenvolvimento Regional through the COMPETE - Operational Program for Competitiveness and by national funds through Fundação para a Ciência e a Tecnologia under the projects FCOMP-01-0124-FEDER-028335, PTDC/BIA-PLA/2291/2012, and PTDC/BIA-FBT/27915/2017. Mass spectrometry was performed at the Proteomics i3S Scientific Platform, with support from the Portuguese Mass Spectrometry Network, integrated in the National Roadmap of Research Infrastructures of Strategic Relevance (ROTEIRO/0028/2013; LISBOA-01-0145-FEDER-022125). LSS was supported by FCT grant SFRH/BD/88406/2012. ARS was supported by national funds and the European social fund (ESF) through the program POCH - grant SFRH/BPD/118147/2016.

Author contributions

The experiments were conceived and designed by LSS, MQA, ARS, and HGC. The experiments were performed by LSS and MQA. The data were analyzed by LSS, MQA, ARS, and HGC. The paper was written by LSS and HGC. All authors read and approved the final manuscript.

Conflicts of interest

The authors declare that the research was conducted in the absence of any commercial or financial relationships that could be construed as a potential conflict of interest.

Declarations of interest

None.

References

[1] N.N. Fancy, A.K. Bahlmann, G.J. Loake, Nitric oxide function in plant abiotic stress, Plant Cell Environ. 40 (2017) 462–472.
[2] M. Yu, L. Lamattina, S.H. Spoel, G.J. Loake, Nitric oxide function in plant biology: a redox cue in deconvolution, New Phytol. 202 (2014) 1142–1156.
[3] J. Astier, C. Lindermayr, Nitric oxide-dependent posttranslational modification in plants: an update, Int. J. Mol. Sci. 13 (2012) 15193–15208.
[4] I. Kovacs, C. Lindermayr, Nitric oxide-based protein modification: formation and site-specificity of protein S-nitrosylation, Front. Plant Sci. 4 (2013).
[5] M. Zaffagnini, M. De Mia, S. Morisse, N. Di Giacinto, C.H. Marchand, A. Maes, S.D. Lemaire, P. Trost, Protein S-nitrosylation in photosynthetic organisms: a comprehensive overview with future perspectives, Biochim. Biophys. Acta 1864 (2016) 952–966.
[6] S. Takahashi, H. Yamasaki, Reversible inhibition of photophosphorylation in chloroplasts by nitric oxide, FEBS Lett. 512 (2002) 145–148.
[7] M.C. Romero-Puertas, N. Campostrini, A. Matte, P.G. Righetti, M. Perazzolli, L. Zolla, P. Roepstorff, M. Delledonne, Proteomic analysis of S-nitrosylated proteins in Arabidopsis thaliana undergoing hypersensitive response, Proteomics 8 (2008) 1459–1469.
[8] C. Lindermayr, G. Saalbach, J. Durner, Proteomic identification of S-nitrosylated proteins in Arabidopsis, Plant Physiol. 137 (2005) 921–930.
[9] M.C. Palmieri, C. Lindermayr, H. Bauwe, C. Steinhauser, J. Durner, Regulation of plant glycine decarboxylase by s-nitrosylation and glutathionylation, Plant Physiol. 152 (2010) 1514–1528.
[10] A. Fares, M. Rossignol, J.B. Peltier, Proteomics investigation of endogenous S-nitrosylation in Arabidopsis, Biochem. Biophys. Res. Commun. 416 (2011) 331–336.
[11] J. Puyaubert, A. Fares, N. Reze, J.B. Peltier, E. Baudouin, Identification of endogenously S-nitrosylated proteins in Arabidopsis plantlets: effect of cold stress on cysteine nitrosylation level, Plant Sci. 215–216 (2014) 150–156.
[12] D. Camejo, C. Romero-Puertas Mdel, M. Rodriguez-Serrano, L.M. Sandalio, J.J. Lazaro, A. Jimenez, F. Sevilla, Salinity-induced changes in S-nitrosylation of pea mitochondrial proteins, J Proteomics 79 (2013) 87–99.
[13] J.C. Begara-Morales, B. Sanchez-Calvo, M. Chaki, C. Mata-Perez, R. Valderrama, M.N. Padilla, J. Lopez-Jaramillo, F. Luque, F.J. Corpas, J.B. Barroso, Differential molecular response of monodehydroascorbate reductase and glutathione reductase by nitration and S-nitrosylation, J. Exp. Bot. 66 (2015) 5983–5996.
[14] J.C. Begara-Morales, B. Sanchez-Calvo, M. Chaki, R. Valderrama, C. Mata-Perez, J. Lopez-Jaramillo, M.N. Padilla, A. Carreras, F.J. Corpas, J.B. Barroso, Dual regulation of cytosolic ascorbate peroxidase (APX) by tyrosine nitration and S-nitrosylation, J. Exp. Bot. 65 (2014) 527–538.
[15] J.K. Abat, R. Deswal, Differential modulation of S-nitrosoproteome of Brassica juncea by low temperature: change in S-nitrosylation of Rubisco is responsible for the inactivation of its carboxylase activity, Proteomics 9 (2009) 4368–4380.
[16] J. Hu, X. Huang, L. Chen, X. Sun, C. Lu, L. Zhang, Y. Wang, J. Zuo, Site-specific nitrosoproteomic identification of endogenously S-nitrosylated proteins in Arabidopsis, Plant Physiol. 167 (2015) 1731–1746.
[17] A.J. Serrato, M.C. Romero-Puertas, A. Lazaro-Payo, M. Sahrawy, Regulation by S-nitrosylation of the Calvin-Benson cycle fructose-1,6-bisphosphatase in Pisum sativum, Redox Biol 14 (2018) 409–416.
[18] J.Z. Liu, J. Duan, M. Ni, Z. Liu, W.L. Qiu, S.A. Whitham, W.J. Qian, S-Nitrosylation inhibits the kinase activity of tomato phosphoinositide-dependent kinase 1 (PDK1), J. Biol. Chem. 292 (2017) 19743–19751.
[19] M. Gietler, M. Nykiel, S. Orzechowski, J. Fettke, B. Zagdanska, Proteomic analysis of S-nitrosylated and S-glutathionylated proteins in wheat seedlings with different dehydration tolerances, Plant Physiol. Biochem. 108 (2016) 507–518.
[20] P.M. Melo, L.S. Silva, I. Ribeiro, A.R. Seabra, H.G. Carvalho, Glutamine synthetase is a molecular target of nitric oxide in root nodules of Medicago truncatula and is regulated by tyrosine nitration, Plant Physiol. 157 (2011) 1505–1517.
[21] Y. Kumada, D.R. Benson, D. Hillemann, T.J. Hosted, D.A. Rochefort, C.J. Thompson, W. Wohlleben, Y. Tateno, Evolution of the glutamine synthetase gene, one of the oldest existing and functioning genes, Proc. Natl. Acad. Sci. U. S. A. 90 (1993) 3009–3013.
[22] G. Pesole, M.P. Bozzetti, C. Lanave, G. Preparata, C. Saccone, Glutamine synthetase gene evolution: a good molecular clock, Proc. Natl. Acad. Sci. U.S.A. 88 (1991) 522–526.
[23] A.R. Seabra, H.G. Carvalho, Glutamine synthetase in Medicago truncatula, unveiling new secrets of a very old enzyme, Front. Plant Sci. 6 (2015) 578.
[24] H. Carvalho, N. Lescure, F. de Billy, M. Chabaud, L. Lima, R. Salema, J. Cullimore, Cellular expression and regulation of the Medicago truncatula cytosolic glutamine synthetase genes in root nodules, Plant Mol. Biol. 42 (2000) 741–756.
[25] P.M. Melo, L.M. Lima, I.M. Santos, H.G. Carvalho, J.V. Cullimore, Expression of the

plastid-located glutamine synthetase of Medicago truncatula. Accumulation of the precursor in root nodules reveals an in vivo control at the level of protein import into plastids, Plant Physiol. 132 (2003) 390–399.
[26] H. Carvalho, L. Lima, N. Lescure, S. Camut, R. Salema, J. Cullimore, Differential expression of the two cytosolic glutamine synthetase genes in various organs of Medicago truncatula, Plant Sci. 159 (2000) 301–312.
[27] H. Carvalho, J. Cullimore, Regulation of glutamine synthetase isoenzymes and genes in the model legume Medicago truncatula, Recent Research Development in Plant Molecular Biology, 2003, pp. 157–175.
[28] A.R. Seabra, C.P. Vieira, J.V. Cullimore, H.G. Carvalho, Medicago truncatula contains a second gene encoding a plastid located glutamine synthetase exclusively expressed in developing seeds, BMC Plant Biol. 10 (2010) 183.
[29] J. Finnemann, J.K. Schjoerring, Post-translational regulation of cytosolic glutamine synthetase by reversible phosphorylation and 14-3-3 protein interaction, Plant J. 24 (2000) 171–181.
[30] L. Lima, A. Seabra, P. Melo, J. Cullimore, H. Carvalho, Phosphorylation and subsequent interaction with 14-3-3 proteins regulate plastid glutamine synthetase in Medicago truncatula, Planta 223 (2006) 558–567.
[31] L. Lima, A. Seabra, P. Melo, J. Cullimore, H. Carvalho, Post-translational regulation of cytosolic glutamine synthetase of Medicago truncatula, J. Exp. Bot. 57 (2006) 2751–2761.
[32] Y.A. Choi, S.G. Kim, Y.M. Kwon, The plastidic glutamine synthetase activity is directly modulated by means of redox change at two unique cysteine residues, Plant Sci. 149 (1999) 175–182.
[33] M.A. Matamoros, N. Fernandez-Garcia, S. Wienkoop, J. Loscos, A. Saiz, M. Becana, Mitochondria are an early target of oxidative modifications in senescing legume nodules, New Phytol. 197 (2013) 873–885.
[34] A.S. Bayden, V.A. Yakovlev, P.R. Graves, R.B. Mikkelsen, G.E. Kellogg, Factors influencing protein tyrosine nitration – structure-based predictive models, Free Radic. Biol. Med. 50 (2011) 749–762.
[35] O. Lamotte, J.B. Bertoldo, A. Besson-Bard, C. Rosnoblet, S. Aimé, S. Hichami, H. Terenzi, D. Wendehenne, Protein S-nitrosylation: specificity and identification strategies in plants, Frontiers in Chemistry 2 (2015).
[36] J.C. Begara-Morales, M. Chaki, R. Valderrama, B. Sanchez-Calvo, C. Mata-Perez, M.N. Padilla, F.J. Corpas, J.B. Barroso, Nitric oxide buffering and conditional nitric oxide release in stress response, J. Exp. Bot. 69 (2018) 3425–3438.
[37] C. Lindermayr, Crosstalk between reactive oxygen species and nitric oxide in plants: key role of S-nitrosoglutathione reductase, Free Radic. Biol. Med. 122 (2018) 110–115.
[38] L. Liu, A. Hausladen, M. Zeng, L. Que, J. Heitman, J.S. Stamler, A metabolic enzyme for S-nitrosothiol conserved from bacteria to humans, Nature 410 (2001) 490–494.
[39] N. Zhan, C. Wang, L. Chen, H. Yang, J. Feng, X. Gong, B. Ren, R. Wu, J. Mu, Y. Li, Z. Liu, Y. Zhou, J. Peng, K. Wang, X. Huang, S. Xiao, J. Zuo, S-Nitrosylation, Targets GSNO reductase for selective autophagy during hypoxia responses in plants, Mol. Cell. 71 (2018) 142–154.e6.
[40] A. Feechan, E. Kwon, B.W. Yun, Y. Wang, J.A. Pallas, G.J. Loake, A central role for S-nitrosothiols in plant disease resistance, Proc. Natl. Acad. Sci. U. S. A. 102 (2005) 8054–8059.
[41] L. Frungillo, M.J. Skelly, G.J. Loake, S.H. Spoel, I. Salgado, S-nitrosothiols regulate nitric oxide production and storage in plants through the nitrogen assimilation pathway, Nat. Commun. 5 (2014) 5401.
[42] C. Rusterucci, M.C. Espunya, M. Diaz, M. Chabannes, M.C. Martinez, S-nitrosoglutathione reductase affords protection against pathogens in Arabidopsis, both locally and systemically, Plant Physiol. 143 (2007) 1282–1292.
[43] V. Lullien, D.G. Barker, P. Delajudie, T. Huguet, Plant gene-expression in effective and ineffective root-nodules of alfalfa (Medicago-Sativa), Plant Mol. Biol. 9 (1987) 469–478.
[44] H.M. Meade, S.R. Long, G.B. Ruvkun, S.E. Brown, F.M. Ausubel, Physical and genetic characterization of symbiotic and auxotrophic mutants of Rhizobium meliloti induced by transposon Tn5 mutagenesis, J. Bacteriol. 149 (1982) 114–122.
[45] A.R. Seabra, L.S. Silva, H.G. Carvalho, Novel aspects of glutamine synthetase (GS) regulation revealed by a detailed expression analysis of the entire GS gene family of Medicago truncatula under different physiological conditions, BMC Plant Biol. 13 (2013) 137.
[46] J.V. Cullimore, A.P. Sims, An association between photorespiration and protein catabolism: studies with Chlamydomonas, Planta 150 (1980) 392–396.
[47] K.A. Broniowska, A.R. Diers, N. Hogg, S-NITROSOGLUTATHIONE, Biochim. Biophys. Acta 1830 (2013) 3173–3181.
[48] S.R. Jaffrey, H. Erdjument-Bromage, C.D. Ferris, P. Tempst, S.H. Snyder, Protein S-nitrosylation: a physiological signal for neuronal nitric oxide, Nat. Cell Biol. 3 (2001) 193–197.
[49] H. Osorio, C.A. Reis, Mass spectrometry methods for studying glycosylation in cancer, Methods Mol. Biol. 1007 (2013) 301–316.
[50] E. Torreira, A.R. Seabra, H. Marriott, M. Zhou, O. Llorca, C.V. Robinson, H.G. Carvalho, C. Fernandez-Tornero, P.J. Pereira, The structures of cytosolic and plastid-located glutamine synthetases from Medicago truncatula reveal a common and dynamic architecture, Acta Crystallogr D Biol Crystallogr 70 (2014) 981–993.
[51] D. Eisenberg, R.J. Almassy, C.A. Janson, M.S. Chapman, S.W. Suh, D. Cascio, W.W. Smith, Some evolutionary relationships of the primary biological catalysts glutamine synthetase and RuBisCO, Cold Spring Harbor Symp. Quant. Biol. 52 (1987) 483–490.
[52] K. Motohashi, A. Kondoh, M.T. Stumpp, T. Hisabori, Comprehensive survey of proteins targeted by chloroplast thioredoxin, Proc. Natl. Acad. Sci. U. S. A. 98 (2001) 11224–11229.
[53] A.R. Jayakumar, M.D. Norenberg, Glutamine synthetase: role in neurological disorders, Adv Neurobiol 13 (2016) 327–350.
[54] B. Gorg, N. Qvartskhava, P. Voss, T. Grune, D. Haussinger, F. Schliess, Reversible inhibition of mammalian glutamine synthetase by tyrosine nitration, FEBS Lett. 581 (2007) 84–90.
[55] K. Raju, P.T. Doulias, P. Evans, E.N. Krizman, J.G. Jackson, O. Horyn, Y. Daikhin, I. Nissim, M. Yudkoff, I. Nissim, K.A. Sharp, M.B. Robinson, H. Ischiropoulos, Regulation of brain glutamate metabolism by nitric oxide and S-nitrosylation, Sci. Signal. 8 (2015) ra68.
[56] J.K. Abat, A.K. Mattoo, R. Deswal, S-nitrosylated proteins of a medicinal CAM plant Kalanchoe pinnata- ribulose-1,5-bisphosphate carboxylase/oxygenase activity targeted for inhibition, FEBS J. 275 (2008) 2862–2872.
[57] E. Baudouin, L. Pieuchot, G. Engler, N. Pauly, A. Puppo, Nitric oxide is formed in Medicago truncatula-Sinorhizobium meliloti functional nodules, Mol. Plant Microbe Interact. 19 (2006) 970–975.
[58] F. Horchani, M. Prevot, A. Boscari, E. Evangelisti, E. Meilhoc, C. Bruand, P. Raymond, E. Boncompagni, S. Aschi-Smiti, A. Puppo, R. Brouquisse, Both plant and bacterial nitrate reductases contribute to nitric oxide production in Medicago truncatula nitrogen-fixing nodules, Plant Physiol. 155 (2011) 1023–1036.
[59] T. Rőszer, Biosynthesis of nitric oxide in plants, in: M.N. Khan, M. Mobin, F. Mohammad, F.J. Corpas (Eds.), Nitric Oxide in Plants: Metabolism and Role in Stress Physiology, Springer International Publishing, Cham, 2014, pp. 17–32.
[60] J. Astier, I. Gross, J. Durner, Nitric oxide production in plants: an update, J. Exp. Bot. 69 (2018) 3401–3411.
[61] A. Sehrawat, R. Deswal, S-nitrosylation analysis in Brassica juncea apoplast highlights the importance of nitric oxide in cold-stress signaling, J. Proteome Res. 13 (2014) 2599–2619.
[62] C. Lindermayr, J. Durner, S-Nitrosylation in plants: pattern and function, J Proteomics 73 (2009) 1–9.
[63] M.C. Romero-Puertas, L.M. Sandalio, Nitric oxide level is self-regulating and also regulates its ROS partners, Front. Plant Sci. 7 (2016) 316.